HHS Public Access

Author manuscript

Biochim Biophys Acta. Author manuscript; available in PMC 2017 September 01.

Published in final edited form as:

Biochim Biophys Acta. 2016 September ; 1862(9): 1521–1532. doi:10.1016/j.bbadis.2016.05.007.

Calcineurin proteolysis in astrocytes: Implications for impaired synaptic function

Melanie M. Pleiss[1], **Pradoldej Sompol**[2], **Susan D. Kraner, Ph.D.**[2], **Hafiz Mohmmad Abdul, Ph.D.**[2], **Jennifer L. Furman, Ph.D.**[1], **Rodney P. Guttmann, Ph.D.**[2], **Donna M. Wilcock, Ph.D.**[2,4], **Peter T. Nelson, M.D., Ph.D.**[2], and **Christopher M. Norris, Ph.D.**[1,2]

Melanie M. Pleiss: melanie.pleiss@uky.edu; Pradoldej Sompol: pradoldej.sompol@uky.edu; Susan D. Kraner: susan.kraner@uky.edu; Hafiz Mohmmad Abdul: hafiz_biochem75@yahoo.com; Jennifer L. Furman: jennifer.furman@utsouthwestern.edu; Rodney P. Guttmann: rguttmann@uwf.edu; Donna M. Wilcock: donna.wilcock@uky.edu; Peter T. Nelson: pnels2@uky.edu; Christopher M. Norris: cnorr2@uky.edu

[1]Department of Pharmacology and Nutritional Sciences, University of Kentucky College of Medicine, Lexington, KY, USA

[2]Sanders Brown Center on Aging, University of Kentucky College of Medicine, Lexington, KY, USA

[3]Department of Psychology, University of West Florida, Pensacola, FL, USA

[4]Department of Physiology, University of Kentucky College of Medicine, Lexington, KY, USA

Abstract

Mounting evidence suggests that astrocyte activation, found in most forms of neural injury and disease, is linked to the hyperactivation of the protein phosphatase calcineurin. In many tissues and cell types, calcineurin hyperactivity is the direct result of limited proteolysis. However, little is known about the proteolytic status of calcineurin in activated astrocytes. Here, we developed a polyclonal antibody to a high activity calcineurin proteolytic fragment in the 45–48 kDa range (ΔCN) for use in immunohistochemical applications. When applied to postmortem human brain sections, the ΔCN antibody intensely labeled cell clusters in close juxtaposition to amyloid deposits and microinfarcts. Many of these cells exhibited clear activated astrocyte morphology. The expression of ΔCN in astrocytes near areas of pathology was further confirmed using confocal microscopy. Multiple NeuN-positive cells, particularly those within microinfarct core regions, also

Correspondence to: Christopher M. Norris, cnorr2@uky.edu.

Competing interests

The authors declare they have no competing interests.

Author's contributions

MMP and SDK performed all human IHC/IF data collection and analysis, interpreted the data, and prepared the manuscript. PS performed the rat injections/collections and the mouse IF data collection and analysis. HMA performed the antibody purification and Western blot data collection and analysis. JLF performed initial IHC troubleshooting. RPG provided equipment for Western blot analysis and guidance in antibody production. PTN provided neuropathologic examination of the human brain biospecimens. DMW provided assistance with IF troubleshooting. CMN conceived of the studies, performed the electrophysiological field recordings, analyzed and interpreted the data, and edited the final manuscript. All authors edited and have approved the final version of this manuscript.

labeled positively for ΔCN. This observation suggests that calcineurin proteolysis can also occur within damaged or dying neurons, as reported in other studies. When a similar ΔCN fragment was selectively expressed in hippocampal astrocytes of intact rats (using adeno-associated virus), we observed a significant reduction in the strength of CA3-CA1 excitatory synapses, indicating that the hyperactivation of astrocytic calcineurin is sufficient for disrupting synaptic function. Together, these results suggest that proteolytic activation of calcineurin in activated astrocytes may be a central mechanism for driving and/or exacerbating neural dysfunction during neurodegenerative disease and injury.

Keywords

calcineurin; proteolysis; astrocytes; Alzheimer's disease; microinfarct

1. Introduction

Mounting evidence suggests that the hyperactivation of the Ca^{2+}/ calmodulin (CaM)-dependent protein phosphatase calcineurin (CN) is a key contributor to the patho-physiologic and clinical symptoms of Alzheimer's disease (AD) and other neurodegenerative disorders [1–8]. The detrimental effects of CN dysregulation may arise through unique alterations in neurons and glial cells [9–11]. In astrocytes and microglia, CN controls immune/inflammatory phenotypes through activation of key transcription factors including nuclear factor of activated T cells (NFAT), nuclear factor κ B (NFκB), and FOXO, among others [9, 12–16]. Previously, we showed that the selective blockade of astrocytic CN/NFAT signaling with the NFAT-inhibitory peptide, VIVIT, suppresses markers of glial activation, alleviates amyloid pathology, and protects against cognitive deficits in experimental models of AD [1, 2, 14] and prevents synapse dysfunction in models of AD and acute brain injury [2, 17]. These results suggest that astrocytes are a key locus of hyperactive CN signaling during the progression of AD. However, little is known about the mechanisms that lead to or sustain aberrant astrocytic CN/NFAT signaling.

Hyperactivation of CN in other cell types, including neurons and cardiomyocytes, can arise from the disruption, or proteolytic removal, of a critical autoinhibitory domain (AID) located near the C-terminus of the CN catalytic subunit (CN A) (for review, see [18]). Normally, when Ca^{2+} levels are low, the AID strongly limits phosphatase activity until it is displaced from the catalytic site by Ca^{2+}/CaM [19]. Proteolytic removal of the AID by the cysteine protease, calpain (CP), can occur after cellular insults and large surges in intracellular Ca^{2+} [20]. Without the AID, CN A is largely, and irreversibly uncoupled from local Ca^{2+} gradients, resulting in elevated phosphatase activity, whether normal levels of Ca^{2+} are restored or not [20]. Many commercial antibodies to the C-terminus of CN A recognize full length CN (FL-CN, ~60 kDa), but fail to detect CN proteolytic fragments (*i.e.* ΔCNs) because the epitope is located in the region that is cleaved away. In contrast, N-terminus antibodies identify both FL-CN and ΔCNs. Use of Western blot techniques and N-terminus CN antibodies has revealed the presence of ΔCNs in whole brain tissue under several neurodegenerative conditions [6, 21–25]. Previous work from our group on human subjects with mild cognitive impairment revealed elevated hippocampal levels of a ΔCN fragment in

the 45–48 kDa range [26]. A similar fragment was generated in mixed (neurons and glia) primary hippocampal cultures, coincident with elevated NFAT activity and frank neuronal degeneration, following treatment with oligomeric amyloid-β peptides. The appearance of ΔCN at early stages of neurologic dysfunction suggests that CN proteolysis is more than a biomarker of neurodegeneration, and may be an antecedent for later neurodegenerative events.

Unfortunately, because of the cell-type heterogeneity of whole brain homogenates, it's nearly impossible to discern where (*i.e.* in what cell type) CN proteolysis is occurring. In immunohistochemical (IHC) applications, N terminus antibodies reveal the presence of CN in multiple cell types, including activated astrocytes [1, 3]. However, it remains unclear whether the labeled CN is of the intact, full-length variety or of the proteolyzed, highly active variety. To resolve this issue, we generated custom antibodies to CN A based on previously identified CP-cleavage sites [20]. One of these antibodies selectively detected a 45–48 kDa fragment (ΔCN) in Western blot assays. IHC investigations of human brain tissue revealed the presence of ΔCN in numerous astrocytes, especially those associated with Aβ deposits and microinfarcts. Adeno-associated virus (AAV)-mediated delivery of a similar ΔCN fragment to hippocampal astrocytes of healthy adult rats caused a reduction in CA1 synaptic strength. Together, the results are consistent with the hypothesis that CN dysregulation in activated astrocytes is attributable, in part, to limited proteolysis. Moreover, the presence of proteolyzed CN in astrocytes appears to be sufficient for disrupting synaptic function, indicating a possibly critical mechanism for synaptic decline in AD and other neurodegenerative conditions.

2. Material and Methods

2.1 ΔCN antibody production and purification

Peptides based on known CP dependent cleavage sites [20] were generated by PrimmBiotech (West Roxbury, MA) and used to inoculate adult rabbits. Antisera from rabbits inoculated with the peptide, ESVLTLK (amino acid sequence immediately upstream of the 48 kDa CN cleavage site) detected a 45–48 kDa fragment in initial Western blot assays. The antisera were then purified using a negative selection approach. In brief, the ESVLTLK peptide was coupled to HiTrapTM NHS-activated HP columns (GE Healthcare, Little Chalfont, United Kingdom) followed by addition of antisera. Antibodies were then eluted and collected according to manufacturer instructions. Following a second round of column-purification, the eluate was aliquoted and frozen for additional Western blot screening.

2.2 Primary cell culture

Primary mixed (astrocytes and neurons) hippocampal cultures were prepared from embryonic day 18 Sprague-Dawley rat pups as described previously [14, 27, 28]. Cells were investigated at between 14 and 21 days in vitro (DIV). To generate CN proteolysis, cultures plated in 35 mm dishes were treated for 24 h with synthetic oligomeric β-amyloid 1-42 (Aβ1-42) peptides (~65 nM) prepared as described in our previous work [1, 26]. Aβ1-42 was delivered in the presence or absence of the CP inhibitor, calpeptin (10 μM), obtained

from EMD Millipore (Gibbstown, NJ). Calpeptin was added to cultures approximately 2 h prior to the addition of Aβ1-42.

2.3 Western blot analysis

At 24 h post- Aβ treatment, cells were homogenized in high sucrose buffer and protein concentration determined using the Lowry method. Samples were loaded onto a Bio-Rad gradient gel (4–20%) with protein concentrations held constant across lanes. Proteins were resolved by electrophoresis and transferred to PVDF membranes for Western blot analysis. Membranes were blocked then incubated overnight at 4°C in the following primary antibodies: 1:3000 anti-CN-Aα (Millipore) and 1:1000 anti-ΔCN (custom). Primary antibodies were labelled with appropriate HRP-conjugated secondary antibodies and detected using the ECL Plus Western Blotting system (GE Healthcare). Relative molecular weights of full length CN and ΔCN were quantified using a Bio Rad Chemidoc XRS Gel imager and Quantity One Software (Hercules, CA).

2.4 Human biospecimens

Post-mortem brain specimens from the amygdala, hippocampus, and superior and middle temporal gyri (SMTG) were obtained from the University of Kentucky Alzheimer's Disease Center (UK-ADC) Tissue Repository. Amygdala and hippocampal specimens from 6 different AD cases and 2 different age-matched control cases were investigated. SMTG biospecimens were from five individual subjects. All subjects were participants in the UK-ADC Autopsy program. Postmortem autopsy intervals for UK-ADC samples, including the ones used in this study, is approximately 3 hours (*e.g.* see [1, 26, 29]). The presence of AD pathology (amyloid plaques and neurofibrillary tangles) and vascular pathology (microinfarcts) in all human cases was confirmed by personnel in the UK-ADC neuropathology core.

2.5 Histology

Paraffin-embedded SMTG sections were cut to ~8 μm thickness and baked overnight at 40°C. Sections were deparaffinized in fresh Xylene and rehydrated through a series of graded alcohols to water. Sections were dipped into Harris's hematoxylin for 4 minutes then rinsed in running water. Following a water rinse, sections were dipped twice into acid alcohol, rinsed in running water, dipped twice into 1% ammonia water, and rinsed in water for 10 minutes. Sections were dipped into Eosin solution for 15–20 seconds and then dehydrated through graded alcohols, cleared using Xylene, and mounted.

2.6 Immunohistochemistry

Amygdala, hippocampal, and SMTG specimens were fixed in 10% formaldehyde, embedded in paraffin, and cut into ~8 μm thick sections. Slides were baked in a 40°C oven overnight, deparaffinized using SafeClear (Fisher Scientific), and rehydrated through a series of graded alcohols to water. Slides were boiled for 10 minutes in Borg Decloaker antigen retrieval solution, pH = 6.0 (Biocare Medical) before blocking endogenous peroxidase activity with 3% hydrogen peroxide + 10% methanol. The slides were blocked (0.1 M Tris buffer with 0.1% Triton X-100 and 2% bovine serum albumin) and incubated overnight at

4°C in the foll owing primary antibodies: 1:25 rabbit polyclonal anti-ΔCN; 1:500 mouse monoclonal anti-CN-Aα (C-terminus) (Sigma);. 1:50 mouse monoclonal anti-Aβ (Vector Laboratories. Secondary antibodies were added at a 1:200 dilution for 1 hour at room temperature as follows: anti-mouse IgG + horse normal serum or anti-rabbit IgG + goat normal serum. Following secondary antibody, signal was amplified with avidin-biotin complex for 1 hour at room temperature and then detected using either DAB or SG substrates (Vector Laboratories). Following dehydration through a series of graded alcohol and clearing (SafeClear), slides were permanently mounted using VectaMount (Vector Laboratories) and coverslipped.

2.7 Immunofluorescence

Amygdala, hippocampal, and SMTG sections were fixed in 4% paraformaldehyde and preserved in sucrose buffer. Slices were cut on a freezing microtome to 50μM thickness. Free-floating sections were blocked (0.1 M Tris buffer with 0.1% Triton X-100 and 2% bovine serum albumin) and incubated overnight at 4°C with primary antibodies including: 1:25 anti-ΔCN; 1:50 anti-GFAP directly conjugated to Alexa 594 (Cell Signaling); 1:100 anti-NeuN (Millipore). After washing, sections were incubated 1:500 in Alexa Fluor 488 or 594 secondary antibodies (Life Technologies). Fluorescent sections were mounted with ProLong Gold Antifade Reagent with DAPI (Molecular Probes) and coverslipped.

2.8 Animals

Adult male Sprague Dawley rats were obtained from Harlan Laboratories (Indianapolis, IN). Rats were held in standard laboratory cages under 12-h light/12-h dark cycles in a pathogen free environment in accordance with University of Kentucky guidelines. The animals had access to food and water ad libitum. All animal procedures were conducted in accordance with the National Institutes of Health Guide for the Care and Use of Laboratory Animals and were approved by University of Kentucky Institutional Animal Care and Use Committees.

2.9 Intrahippocampal delivery of adeno-associated virus (AAV)

cDNA encoding the first 398 amino acids of the CN Aα isoform (ΔCN), which lacks the Ca^{2+}/CaM binding domain and the AID [30], was subcloned into the polylinker site of a hybrid pCI vector containing IRES2-DsRed-Express (Clontech, Mountain View, CA). IRES-DsRed2 (control construct) or ΔCN-IRES-DsRed2 were then inserted into pAAV2-Gfa104-EGFP (University of Pennsylvania Vector core) in place of EGFP. High titer (10^{12} IFU/mL) AAV vectors (AAV-Gfa104-DsRed and AAV-Gfa104-ΔCN) were then generated in the University of Kentucky Vector core using an AAV5 helper plasmid and HEK293 cells. The Gfa104 promoter has been characterized previously, and has been shown to drive transgene expression selectively in astrocytes of intact animals [31, 32], similar to that seen with the Gfa2 promoter (e.g. see [17]).

Rats were placed in a stereotaxic frame (David Kopf Instruments Tujunga, CA) and anesthetized with isoflurane (2.5%) throughout the surgery process. For each rat, AAV-Gfa104-DsRed and AAV-Gfa104-ΔCN were loaded into separate microinjectors and delivered into alternate hemispheres, such that one hippocampus was treated with Gfa104-DsRed and the other hippocampus was treated with Gfa104-ΔCN. Each hemisphere was

injected with 4 μL of AAV (10^{12} IFU/mL) at 0.2 μL/min. Injection coordinates were −3.8mm anteroposterior and +1.8mm mediolateral relative to bregma, and −1.8mm dorsoventral relative to dura. DsRed visualization in formaldehyde-fixed tissue sections was achieved using a rabbit polyclonal antibody to red fluorescent protein (Abcam) and Alexa Fluor secondary antibodies as described above for human sections.

2.10 Hippocampal slice electrophysiology

At 4 months after AAV injection, rats were euthanized under CO_2 anesthesia and decapitated. Brains were rapidly removed and placed in ice-cold, oxygenated (95% O2, 5% CO2) artificial cerebrospinal fluid (ACSF) containing (in mM) 124 NaCl, 2 KCl, 1.25 KH_2PO_4, 2 $MgSO_4$, 0.5 $CaCl_2$, 26 $NaHCO_3$, and 10 dextrose (pH 7.4). Brains were hemisected and glued to a specimen mounting block and submerged in oxygenated, ice-cold ACSF. Brains were then sectioned coronally into ~400 μm slices using a Vibratome® 1000 (Leica Biosystems, Buffalo Grove, IL) and transferred to a custom interface holding chamber [33] and incubated with warmed (32° C) oxygenated ACSF containing 2 mM $CaCl_2$ until electrophysiological recordings (usually 1.5–5 h).

Slices were transferred to a Kerr Tissue Recording system (Kerr Scientific Instruments, Christchurch, New Zealand) and submerged in warmed (~32° C) oxygenated ACSF containing 2mM $CaCl_2$ and 2mM $MgSO_4$. Schaffer collaterals were activated with a bipolar stainless steel electrode located in *stratum radiatum*. Stimulus intensity was controlled by a constant current stimulus isolation unit (World Precision Instruments, Sarasota, FL), and stimulus timing was controlled by LabChart 8 software (ADInstruments Inc., Colorado Springs, CO). Field potentials were recorded in CA1 *stratum radiatum* using a Ag/AgCl wire located ~1–2 mm from the stimulating electrode. Field potentials were amplified 100X and digitized at 10kHz using the Kerr Tissue Recording System amplifier and a 4/35 PowerLab analog-to-digital converter (ADInstruments). To assess basal synaptic strength, 100 μs stimulus pulses were given at 12 intensity levels (range 25–500 μA) at a rate of 0.1 Hz. Five field potentials at each level were averaged, and measurements of fiber volley (FV) amplitude (in mV) and excitatory postsynaptic potential (EPSP) slope (mV/ms) were performed offline using LabChart 8 software. Synaptic strength curves were constructed by plotting EPSP slope values against FV amplitudes for each stimulus level. Curves were fit with a three parameter sigmoidal equation using SigmaPlot 12 software (Systat Software Inc. San Jose, CA) [34]. Curve parameters included maximal EPSP amplitude (Max), curve slope, and the FV amplitude associated with the half-maximal EPSP amplitude (half-Max). Maximal synaptic strength for each slice was also estimated by taking the maximal EPSP slope amplitude during the input/output curve and dividing by the corresponding FV amplitude. To estimate population spike (PS) threshold, the EPSP slope amplitude at which a population spike first appeared in the ascending phase of the field potential was calculated and averaged across five successive trials at the spike threshold stimulation level.

2.11 Statistics

For slice electrophysiology studies, one to three slices from each hemisphere (either the Gfa104-DsRed or the Gfa104-ΔCN-treated hemisphere) were analyzed. Synaptic measures

were averaged across all slices within each hemisphere and these averaged values were compared across hemispheres using paired T-tests, with significance set at $p < 0.05$.

3. Results

3.1 Custom antibody shows greater selectivity to a ΔCN fragment

The CN A subunit is a 521 amino acid protein consisting of a catalytic domain and an autoinhibitory domain (AID), as well as binding sites for the CN B regulatory subunit and Ca^{2+}/calmodulin (Ca^{2+}/CaM) ([30, 35], see Figure 1). Proteolysis of CN A near the carboxy-terminus by calpains results in the disruption or removal of the AID leading to reduced Ca^{2+} sensitivity and constitutive phosphatase activity [20]. Calpain-mediated generation of 45 and 48 kDa ΔCN fragments are found at elevated levels in human brain tissue during cognitive decline, are triggered by oligomeric Aβ, and are causatively linked to greater CN signaling and neurodegeneration [20, 26].

CN A antibodies that target epitopes between amino acid residues 425 and 521 (*i.e.* C terminus antibodies) recognize full length CN (FL-CN), but do not detect ΔCN fragments and may therefore fail to identify important pathological changes in CN regulation. In contrast, N terminus-directed antibodies identify CN proteolysis in Western blot applications, but do not distinguish between FL-CN and ΔCN in immunohistochemical applications, making it difficult to pinpoint where CN proteolysis occurs in a heterogeneous cell population. We therefore set out to make new antibody reagents with greater selectivity to ΔCN, relative to FL-CN. Peptides composed of amino acids found immediately upstream of calpain-dependent cleavage sites [20] were used to immunize rabbits (Figure 1). Antisera generated by immunization with the ESVLTLK peptide, found immediately upstream from lysine 424, revealed a 45–48 kDa band in preliminary Western blots (not shown) and was therefore subjected to further affinity purification (see Methods) to obtain ΔCN antibodies (Figure 1A,B). We then performed Western blots (Figure 1C) on whole cell lysates obtained from rat primary mixed (neurons + glia) hippocampal cultures exposed to oligomeric Aβ peptides (65 nM for 24 h) to stimulate CN proteolysis, as described in our earlier work [26]. The same samples were processed in parallel for Western blot using a commercially available N terminus CN antibody for comparison. Both antibodies showed diffuse labeling in the 70–75 kDa range. However, unlike the ΔCN antibody, the N terminus antibody showed a prominent band in the 60 kDa range (where FL-CN is found) in untreated cultures, along with lower molecular weight bands between 25 and 37 kDa (Figure 1C, lane 5). Both antibodies revealed bands in the 45–48 kDa range when cultures were treated with oligomeric Aβ (Figure 1C, lanes 2 and 6), the appearance of which was blocked by co-application of the calpain inhibitor, calpeptin (Figure 1C, lanes 3 and 7), but not by the caspase inhibitor Z-YVAD (Figure 1C, lanes 4 and 8). Together, these data demonstrate that, relative to the N-terminus antibody, the ΔCN antibody shows far greater selectivity to calpain-dependent CN proteolytic products in the 45–48 kDa range.

3.2 Astrocytes in AD brain tissue are labeled intensely with the ΔCN antibody

Western blot analyses have shown elevated levels of ΔCN in brain homogenates from human subjects with mild-cognitive impairment [26] or AD [6], relative to age-matched non-

demented human subjects. Though CN is primarily found in neurons, it can also appear at high levels in activated astrocytes during injury and disease, especially around Aβ deposits [1, 3, 36]. To determine if ΔCN is found in activated astrocytes, we immunohistochemically (IHC) labeled human postmortem brain sections (encompassing the amygdala and overlying entorhinal cortex) from subjects with confirmed AD (see Methods). These brain regions show high levels of CN expression in healthy adult animals [37, 38], and exhibit extensive amyloid and neurofibrillary tangle pathology during AD [39]. Concurrent with AD-related pathological changes, these brain regions also show widespread GFAP labeling indicative of gliosis, or astrocyte activation ([40] and see Figure 2A).

In IHC applications, the ΔCN antibody provided excellent labeling intensity with low background (Figure 2B–E). With rare exceptions (see arrow in Figure 2E), most of the labeled cells exhibited a clear astrocyte morphology, with thick ramified processes, characteristic of astrocyte activation (Figure 2B, 2C). Unlike the GFAP antibody, which provided labeling across most of the tissue (Figure 2A), the ΔCN antibody generally provided only faint labeling, except for numerous discrete regions characterized by astrocyte “clusters” (Figure 2B and C). Cells within these clusters showed intense labeling, which appeared throughout the soma and usually throughout several major processes (Figure 2C). Many of the most intensely labeled astrocytes were in close juxtaposition to blood vessels (Figure 2D, arrow). Costaining with an antibody to Aβ showed that many ΔCN-positive clusters occurred around extracellular amyloid plaques (Figure 2E), suggesting that the proteolysis of CN in astrocytes is strongly coupled to amyloid pathology, consistent with previous reports [6, 26].

In contrast to the conspicuous labeling patterns shown in human AD tissue, staining with the ΔCN antibody appeared much less prominent in the amygdala of age-matched control subjects (Supplementary Figure 1). We also observed sparse labeling when tissue sections were incubated with the ΔCN antibody alone (*i.e.* without secondary antibody, Supplementary Figure 1) or with the ΔCN antibody plus ESVLTLK blocking peptide (Figure 2F and 2G). These results demonstrate that antibody labeling was specific.

Finally, to confirm that ΔCN is definitively expressed in astrocytes, AD amygdala sections were co-labeled with a GFAP antibody and confocal microscopy was used to assess co-localization. As illustrated in Figures 2H–K, GFAP and ΔCN were co-localized in numerous cells. Note, however, that ΔCN was not present in all GFAP positive cells. For instance, arrowheads in Figures 2H–J show two immediately adjacent astrocytes, with one cell expressing ΔCN and the other cell apparently devoid of ΔCN (also see Figure 2K). These images, along with the immunohistochemical evidence shown in Figures 2B–2E highlight the heterogeneous nature of CN proteolysis in astrocyte populations associated with AD pathology.

As mentioned, a relatively small number of ΔCN-positive cells in the amygdala exhibited a clear neuronal morphology (see Figure 2E, arrow). As a further attempt to explore neuronal labeling with the ΔCN antibody, we investigated hippocampal sections using both immunohistochemistry and confocal microscopy. The hippocampus is advantageous for immunohistochemical investigations because its neurons are densely packed into discrete

layers and are easy to identify, even in unstained tissue. Moreover, studies from our group have reported signs of hyperactive CN signaling in the hippocampus during the progression of AD [1, 26].

As shown in Figures 3A and B, neurons in the CA1 and dentate granule layers of AD subjects showed abundant expression of the full length form of CN [37, 38], as revealed using a commercial antibody to the CN carboxyl terminus. The ΔCN antibody also labeled neurons, albeit more sparsely (Figure 3C and 3D) than the commercial antibody. Similar to amygdala sections, hippocampal tissue from control subjects provided little to no labeling (Supplemental Figure 1). When present, ΔCN expression was generally limited to the somal and proximal apical dendritic regions (for CA1 pyramidal neurons), and tended to be faint, even when other structures in the same region, including perivascular elements (Figure 3C) and astrocytes (inset, Figure 3D), were strongly labeled. In many neurons, ΔCN co-localized with the nuclear marker, NeuN, which is consistent with earlier work that found elevated levels of proteolyzed CN in nuclear extracts from AD subjects [6]. Thus, while activated astrocytes appear to provide the most striking ΔCN labeling patterns associated with AD, these cells are not the only source for CN proteolysis.

3.3 Association of ΔCN with microinfarcts

In addition to AD, ΔCN fragments have been observed in a number of other neurodegenerative conditions, particularly those caused by vasculature disruption and/or occlusion [23–25]. Vascular pathology is highly co-morbid with AD pathology and likely exacerbates cognitive decline with the progression of AD [41–47]. Mounting evidence suggests that microinfarcts are among the most common and insidious contributors to vascular cognitive impairment and dementia (VCID) [48, 49]. Moreover, microinfarcts are commonly enveloped by activated astrocytes [50, 51].

To determine whether the appearance of ΔCN coincides with vascular disruption, we investigated cortical brain sections from subjects with confirmed microinfarct pathology. Figure 4A–E shows ΔCN labeling in SMTG sections from a 90 year old human subject with multiple microinfarcts, but little-to-no AD pathology (Braak stage II). At low magnification, several discrete regions show very intense ΔCN labeling (Figure 4A). The region marked by the arrowhead in Figure 4A is shown at higher magnification in an H&E labeled serial section in Figure 4B and confirms the presence of a microinfarct approximately 400 μm in greatest dimension (approximate center shown with arrow). This microinfarct is surrounded by numerous cells intensely labeled for ΔCN (Figure 4C), many of which exhibit clear activated astrocyte histomorphology (Figures 4D–E). When the ΔCN antibody was delivered in the presence of the ESVLTLK peptide (Figure 4F and 4G), cellular labeling was greatly diminished, confirming binding specificity. Interestingly, ΔCN-positive microinfarcts were not labeled with a commercial C-terminus-directed antibody that selectively detects full length CN (Figure 4H and I). Note, however, that the C-terminus antibody does label neurons within the same brain section (Supplemental Figure 2). Thus, microinfarcts appear to be more strongly associated with proteolyzed CN than with full-length CN.

Confocal micrographs showed that ΔCN was associated with both activated astrocytes and neurons in the immediate vicinity of microinfarcts (Figure 5). ΔCN localization to astrocytes

was most prominent around the microinfarct core, with expression diminishing with increasing distance from the injury (Figure 5A–5D). For neurons, ΔCN was most highly expressed within the microinfarct core, though many ΔCN/NeuN positive cells could also be found outside the core as well (Figure 5E–H). Together; these observations demonstrate that CN proteolysis can occur in the immediate vicinity of small vessel pathology in the human brain.

3.4 Forced overexpression of ΔCN in astrocytes of intact rats disrupts synaptic function

The consequences of CN proteolysis in neurons have been investigated in many different model systems [18]. Conversely, little is known about the functional outcomes of CN proteolysis in astrocytes. Hyperactivation of CN signaling in astrocytes has been linked to the elevated expression of inflammatory mediators, impaired glutamate regulation, Aβ production, and altered astrocytic Ca^{2+} dynamics [3, 12–14, 18, 52, 53]. Using adeno-associated virus (AAV) vectors, equipped with astrocyte specific promoters, we have shown that the selective inhibition of astrocytic CN/NFAT signaling provides numerous beneficial effects in a mouse model of AD [2], and a rat model of traumatic brain injury [17]. These results suggest that hyperactivation of CN in astrocytes can mediate and/or exacerbate pathophysiological processes.

One of the primary responsibilities of astrocytes is to regulate synaptic transmission and plasticity [54]. Since we previously found that inhibition of astrocytic CN/NFAT signaling protects multiple synaptic properties, we sought to test whether the presence of ΔCN in astrocytes is sufficient to drive synaptic dysfunction. AAV2/5 vectors expressing ΔCN-DsRed2 or DsRed2 alone (control vector) were injected into the hippocampus of adult rats. One hemisphere received ΔCN and the other hemisphere received DsRed2 control vector (Figure 6A). The ΔCN used here lacks the CN AID, is nearly identical in size to the ΔCN fragment found in human AD brain (Figures 2 and 3, and see [2]), and shows increased phosphatase activity when expressed in many different cell types [55–58], including primary astrocytes [14]. Both ΔCN and DsRed2 were transcriptionally regulated by a truncated human GFAP promoter (Gfa104), which provides astrocyte-specific expression [31, 32]. Using confocal microscopy and/or immunodepletion assays, we previously showed that AAV-mediated expression of EGFP was driven exclusively in astrocytes (in mice and rats) when a similar Gfa2 promoter was used [2, 17]. Consistent with these observations, immunofluorescent labeling of the DsRed2 tag in the present study was limited to astrocytes and showed no co-localization with the neuron-specific protein MAP2b (Figure 6B).

At 4 months post-AAV injection, brain slices from both hemispheres were harvested and processed in parallel for the electrophysiological assessment of basal CA3-CA1synaptic strength. Field EPSP slopes were recorded in CA1 *stratum radiatum* and plotted against corresponding FV amplitudes at 12 different stimulus intensities to generate synaptic strength curves (Figure 6C, D). Compared to slices from the DsRed2 control vector-treated hemisphere, slices from the ΔCN-treated side exhibited depressed synaptic strength curves (Figure 6D) with a corresponding reduction in the maximal EPSP/FV ratio ($p < 0.05$, Figure 6E). Further analyses of synaptic strength curve parameters revealed a significant reduction in the maximal EPSP amplitude ($p < 0.05$), but did not find any differences in the slope of the

curve or in the FV amplitude necessary for half-maximal EPSP amplitude (Figure 6F). Finally, while the evoked field EPSP was reduced in slices from the ΔCN-treated hemisphere, these slices were also generally more excitable as indicated by a reduced population spike (PS) threshold (Figure 6G). A similar reduction in the PS threshold has been reported in APP/PS1 mice [2] and may be indicative of neuronal hyperexcitability. Together, these results suggest that the presence of ΔCN in astrocytes is sufficient to drive synaptic dysfunction in intact animals.

4. Discussion

CN proteolytic fragments show abnormally high levels of phosphatase activity under resting Ca^{2+} levels and are associated with numerous forms of neurologic injury and disease [18]. Using a novel antibody generated to the ΔCN proteolytic fragment, the present study has provided some of the first evidence that CN proteolysis can occur extensively in astrocytes associated with AD and small vessel pathology. Furthermore, overexpression of the ΔCN fragment in astrocytes of otherwise healthy adult animals causes synaptic deficits. The results demonstrate that proteolysis may be an important source of CN dysregulation in astrocytes leading to altered astrocyte function and neural dysfunction with the progression of neurodegenerative disease.

4.1 Importance of antibody selection for assessing CN expression/activity in disease

The proteolysis of CN was first shown under *in vitro* conditions, but has subsequently been demonstrated to occur in intact nervous tissue after cellular insult [20, 21, 23–26]. Using an antibody directed to the N terminus of CN A, Wu et al [20] showed that at least three distinct CN A fragments are generated *in vivo* in response to cellular injury and high levels of calpain activity. The 48 and 45 kDa fragments generated by calpain-dependent proteolysis are fully-functional enzymes that show high activity at low (resting) Ca^{2+} levels due to the absence of an AID that normally keeps CN activity in check. High levels of CN proteolysis can dramatically alter cellular function and viability [20, 26, 58], which highlights the importance of choosing the appropriate antibody to investigate CN functions in CNS injury and disease. In particular, C-terminus directed antibodies to CN A only detect full length CN and may give the impression that CN expression is reduced, rather than proteolytically activated, under neurodegenerative conditions. The use of C terminus antibodies may explain why early reports observed reductions in CN A levels and activity in AD tissue [59–62].

While N-terminus antibodies are useful in Western blot applications for determining the extent of CN proteolysis in whole brain tissue, they do not specify which cell types give rise to CN proteolysis, nor do they determine whether proteolysis occurs selectively in the close proximity of specific pathological markers. Furthermore, because of the vast cellular heterogeneity of the CNS, changes in proteolysis for any one cell type may be masked or diluted in biochemical analyses of whole tissue homogenates. This problem severely limits mechanistic insights into the downstream consequences of CN proteolysis, primarily because CN is expressed in many different cell types [1, 3, 36–38, 63], each of which can use CN for unique functions. For example, when expressed in neurons using gene delivery

techniques, ΔCN causes alterations in synaptic function, Ca^{2+} channel dysregulation, degeneration of neurites, and apoptosis [7, 18, 36, 39, 48–50].

Astrocytes may also be an important source for CN dysregulation [10], which is notable given the increasing attention astrocytes have received for their contributions to neurologic dysfunction during aging, injury, and disease [64–67]. Overexpression of ΔCN in astrocytes leads to the production and release of a variety of immune factors (*e.g.* cytokines and chemokines) linked to glial activation and neuroinflammation [3, 13, 14]. While many of these cell-specific processes arise in neurodegenerative diseases, and are blocked by both calpain and CN inhibitors [18], it has been unclear if (and to what extent) CN proteolysis actually occurs in these cell types during the disease process.

The ΔCN antibody was designed with the intent to identify the cellular source for CN proteolysis in diseased and/or injured brain tissue. This antibody showed much greater selectivity to calpain-generated CN fragments than to full-length CN (Figure 1C) in Western blot applications and was associated with high-signal to background labeling in IHC applications (*e.g.* see Figures 2 and 4). When incubated with postmortem human brain sections from confirmed AD cases, the ΔCN antibody provided intense labeling of astrocyte clusters, many of which were in close juxtaposition to Aβ deposits and/or blood vessels (Figure 2). Previously, we observed a similar co-localization of CN to activated astrocytes in amyloidogenic mice and human AD brain tissue using N-terminus antibodies, which identify both full length and proteolyzed CN [1, 3]. The findings of the present study suggest that the elevated activity of CN and/or CN-dependent signaling mediators (*e.g.* NFAT) reported earlier for AD mouse models and human AD cases [1, 4, 6, 26] may arise, at least partly, from the calpain-dependent proteolysis of CN in astrocytes.

4.2 ΔCN and Microinfarcts

ΔCN labeling was also particularly intense for astrocytes in human cases characterized by extensive vascular pathology (Figure 4). Microinfarcts, in particular, are increasingly recognized as a key mechanism for dementia [48, 49]. Though etiologically distinct from AD pathology, microinfarcts and other forms of vascular pathology show high comorbidity with AD, where they appear to exacerbate neurodegenerative processes and hasten cognitive decline [41–47]. Microinfarcts are often defined by extensive gliosis surrounding the core, including profound astrocyte activation [50, 51]. Similar to Aβ plaque-associated astrocytes, we found that activated astrocytes surrounding microinfarcts were intensely labeled with the ΔCN antibody (Figure 4), suggesting that small vascular pathologies can result in aberrant CN proteolysis, which may, in turn, contribute to further glial activation and/or elevated levels of harmful neuroinflammatory factors [14]. While many of the ΔCN-labeled cells around microinfarcts had activated astrocyte morphology, it’s possible that GFAP-negative astrocytes, activated microglia, and/or infiltrating immune cells are also an important source of ΔCN. Microglia, in particular, express numerous CN-dependent substrates, including NFATs that play key roles in cytokine production and neuroinflammation [8, 23, 68–70]. Other cells relevant to the vasculature, such as microvascular pericytes, can express high levels of NFAT4 [71], which is intriguing given that ΔCN was also commonly observed in or around microvessels in the present study.

In addition to glial cells, we also observed ΔCN labeling in neurons, especially within close proximity to microinfarcts (Figure 5B). NeuN- ΔCN colocalization appeared most extensive within the microinfarct core region, which may be subject to marked hypoxic damage [72]—a well-characterized stimulus for CN proteolysis in brain tissue [24, 25]. As mentioned, ΔCN expression in neurons has been shown to activate both necrotic and apoptotic signaling pathways [20, 58], suggesting that the neuronal expression of ΔCN within and near microinfarcts may also be a major contributor to neurodegeneration associated with vascular damage. Additional work directed at identifying all of the different cell types expressing ΔCN following microvessel damage and how CN proteolysis in each cell type specifically contributes to neural function/dysfunction should provide important insights into the pathophysiology of AD and VCID.

4.3 ΔCN in Astrocytes and synapses

One of the major functions of astrocytes is to promote the structural and functional integrity of synaptic contacts [54]. Deficits in synaptic function are usually found in animal models characterized by extensive astrocyte activation [2, 73, 74], suggesting that activated astrocytes directly damage and/or lose the capacity to protect synapses. We previously showed that the blockade of astrocytic CN/NFAT signaling, using AAV-Gfa vectors, ameliorated synaptic deficits in both basal synaptic transmission and plasticity and normalized the PS threshold in APP/PS1 mice [2]. Similar levels of synaptoprotection were observed in brain-injured rats treated with the same AAV reagents [17]. Consistent with these findings, the present study found that hippocampal synaptic strength was compromised in healthy adult rats following the forced overexpression of ΔCN in astrocytes. Together, the results are consistent with the possibility that proteolytic activation of CN in activated astrocytes is a crucial causative mechanism for the deterioration of synaptic function. However, our results do not rule out the possibility that full-length CN could mediate similar effects (in the absence of proteolysis), if the phosphatase was activated at high levels by normal binding to Ca^{2+}/calmodulin.

While the present study did not address how astrocytic CN activity disrupts synaptic function, there are many possible mechanisms that will need to be systematically investigated. For instance, CN signaling pathways help drive the production of numerous immune factors, including tumor necrosis factor and other cytokines, which are implicated in chronic neuroinflammation [14, 75–77] and widely regarded as causal factors of synaptic decline in animal models of aging, injury, and AD [74, 78, 79]. Synaptic function is also strongly modulated by a variety of releasable factors (*e.g.* SPARC/SPARC-L, C3, and ephrin/Eph receptors) [80–82], which are produced in activated astrocytes [83–85] and sensitive to CN/NFAT activity [3, 17], while other toxins, such as glutamate and Aβ peptides, can be released from activated astrocytes via the CN-dependent downregulation of glutamate transporters [1, 14] and the upregulation of β-secretases [2, 53], respectively. But, regardless of the specific cellular mechanism, our data provide proof-of-concept that CN hyperactivity in astrocytes, especially in areas of amyloid and vascular pathology (as shown with the ΔCN antibody, see Figures 2–4), can have deleterious effects on synapses. Whether the proteolysis of CN is directly linked to the striking synapse loss that occurs with AD [86–88] and VCID [89] is still unknown and will need to be determined.

4.4 ΔCN in Astrocytes: Deleterious vs Beneficial Effects on Neural Function

The electrophysiological findings in the present study are consistent with numerous studies that have found a deleterious role of CN signaling in rodent models of aging [3, 90], AD [2–6, 91–93], and injury [17, 20, 21, 24, 25]. The data provided here also directly supports our previous work [2, 17] and work from others [15] showing that astrocyte-specific inhibition of CN signaling results in improved neuronal viability, synaptoprotection, and/or improved cognition. However, these results are apparently in disagreement with another study by the Torres-Aleman lab that showed a number of neurologic benefits in amyloidogenic mice when ΔCN was overexpressed in astrocytes (see Fernandez et al., 2012, [16]). The reason(s) for this discrepancy is not immediately clear. In many tissues, overexpression of ΔCN is associated with cellular toxicity (*e.g.* see [20, 58]. It's therefore possible that the overexpression of ΔCN, in the context of an already toxic environment (*i.e.* high amyloid levels), leads to the death of activated astrocytes. The end result may be beneficial, if activated astrocytes are having a deleterious impact on neural function. Though we observed no evidence for astrocyte deterioration in adult rats treated with AAV-Gfa vectors, the viability of ΔCN -expressing astrocytes should be closely monitored in future studies, especially when ΔCN is expressed in animal models where neuropathology is already extensive. Alternatively, the beneficial vs. detrimental effects of ΔCN could be a further indication of the highly heterogeneous nature of astrocytes both within and across different brain regions. In the present study, forced overexpression of ΔCN was limited to astrocytes in the hippocampus, which is also where we observed beneficial effects of CN/NFAT inhibition using AAV-Gfa vectors [2, 17]. In contrast, Fernandez et al 2012 induced ΔCN expression in astrocytes across the entire forebrain. The specific outcome of ΔCN expression may therefore depend critically on the brain region examined. It's also possible that ΔCN generates some neurologic benefits, including improved cognition, at the cost of other functions, like synaptic transmission and plasticity, though this would be contrary to numerous other studies where synaptic deficits and cognitive impairments run in parallel. Finally, it is interesting to note that a more recent study by the Torres-Aleman lab [15] reported a number of functional benefits in AD transgenic mice following treatment with reagents that disrupt astrocytic CN signaling, which is more consistent with our present findings and previous research. Regardless, it would appear that astrocytic CN signaling is highly complex and additional research will be necessary to fully characterize the molecular, cellular, and behavioral phenotypes of animals that show elevated levels of ΔCN in brain astrocytes.

5. Conclusions

The increasing number of reports showing neuroprotective effects of CN inhibitors in experimental models, coupled with recent epidemiological evidence showing lower dementia rates in human transplant patients treated with CN inhibitors [5], strongly support a critical role for aberrant CN signaling in AD and other neurodegenerative disorders. The findings reported here suggest that CN proteolysis in astrocytes may be a specific mechanism for CN dysregulation and a critical component of abnormal glial cell activation leading to neurodegeneration and dementia. Though additional work will be necessary to more extensively characterize the role of CN proteolysis in glial signaling, the present

results suggest that interventions that limit CN proteolysis may provide an effective strategy for treating AD, vascular dementia, and other forms of neurodegenerative disease.

Supplementary Material

Refer to Web version on PubMed Central for supplementary material.

Acknowledgments

This work was supported by National Institutes of Health Grants R01AG027297, F31AG047762, P01NS058484, P30AG028383; PhRMA Foundation Pre-Doctoral Fellowships, an award from the Kentucky Spinal Cord and Head Injury Research Trust (12-10A) and a gift from the Hazel-Embry Research Fund (CMN). We thank Ela Patel, Elizabeth Head, Tiffany Sudduth, and Adam Bachstetter for technical assistance.

Abbreviations

ΔCN	calcineurin proteolytic fragment
AD	Alzheimer's disease
AID	autoinhibitory domain
IHC	immunohistochemistry
Aβ	beta-amyloid
SMTG	superior and middle temporal gyri
NeuN	neuronal-specific nuclear protein
DAB	3,3′-diaminobenzidine
CaM	calmodulin
N-terminus	amino-terminus
C-terminus	carboxy-terminus
FL-CN	full length calcineurin
GFAP	glial fibrillary acidic protein
CA1	*cornus ammonis* 1
H&E	hematoxylin & eosin
CNS	central nervous system
VCID	vascular cognitive impairment and dementia

References

1. Abdul HM, Sama MA, Furman JL, Mathis DM, Beckett TL, Weidner AM, Patel ES, Baig I, Murphy MP, LeVine H 3rd, Kraner SD, Norris CM. Cognitive decline in Alzheimer's disease is associated

with selective changes in calcineurin/NFAT signaling. J Neurosci. 2009; 29:12957–12969. DOI: 10.1523/JNEUROSCI.1064-09.2009 [PubMed: 19828810]

2. Furman JL, Sama DM, Gant JC, Beckett TL, Murphy MP, Bachstetter AD, Van Eldik LJ, Norris CM. Targeting astrocytes ameliorates neurologic changes in a mouse model of Alzheimer's disease. J Neurosci. 2012; 32:16129–16140. DOI: 10.1523/JNEUROSCI.2323-12.2012 [PubMed: 23152597]
3. Norris CM, Kadish I, Blalock EM, Chen KC, Thibault V, Porter NM, Landfield PW, Kraner SD. Calcineurin triggers reactive/inflammatory processes in astrocytes and is upregulated in aging and Alzheimer's models. J Neurosci. 2005; 25:4649–4658. DOI: 10.1523/JNEUROSCI.0365-05.2005 [PubMed: 15872113]
4. Reese LC, Zhang W, Dineley KT, Kayed R, Taglialatela G. Selective induction of calcineurin activity and signaling by oligomeric amyloid beta. Aging Cell. 2008; 7:824–835. DOI: 10.1111/j.1474-9726.2008.00434.x [PubMed: 18782350]
5. Taglialatela G, Rastellini C, Cicalese L. Reduced Incidence of Dementia in Solid Organ Transplant Patients Treated with Calcineurin Inhibitors. J Alzheimers Dis. 2015; 47:329–333. DOI: 10.3233/JAD-150065 [PubMed: 26401556]
6. Wu HY, Hudry E, Hashimoto T, Kuchibhotla K, Rozkalne A, Fan Z, Spires-Jones T, Xie H, Arbel-Ornath M, Grosskreutz CL, Bacskai BJ, Hyman BT. Amyloid beta induces the morphological neurodegenerative triad of spine loss, dendritic simplification, and neuritic dystrophies through calcineurin activation. J Neurosci. 2010; 30:2636–2649. DOI: 10.1523/JNEUROSCI.4456-09.2010 [PubMed: 20164348]
7. Rojanathammanee L, Floden AM, Manocha GD, Combs CK. Attenuation of microglial activation in a mouse model of Alzheimer's disease via NFAT inhibition. J Neuroinflammation. 2015; 12:42.doi: 10.1186/s12974-015-0255-2 [PubMed: 25889879]
8. Rojanathammanee L, Puig KL, Combs CK. Pomegranate polyphenols and extract inhibit nuclear factor of activated T-cell activity and microglial activation in vitro and in a transgenic mouse model of Alzheimer disease. J Nutr. 2013; 143:597–605. DOI: 10.3945/jn.112.169516 [PubMed: 23468550]
9. Abdul HM, Furman JL, Sama MA, Mathis DM, Norris CM. NFATs and Alzheimer's Disease. Mol Cell Pharmacol. 2010; 2:7–14. [PubMed: 20401186]
10. Furman JL, Norris CM. Calcineurin and glial signaling: neuroinflammation and beyond. J Neuroinflammation. 2014; 11:158.doi: 10.1186/s12974-014-0158-7 [PubMed: 25199950]
11. Reese LC, Taglialatela G. A role for calcineurin in Alzheimer's disease. Curr Neuropharmacol. 2011; 9:685–692. DOI: 10.2174/157015911798376316 [PubMed: 22654726]
12. Canellada A, Ramirez BG, Minami T, Redondo JM, Cano E. Calcium/calcineurin signaling in primary cortical astrocyte cultures: Rcan1-4 and cyclooxygenase-2 as NFAT target genes. Glia. 2008; 56:709–722. DOI: 10.1002/glia.20647 [PubMed: 18293408]
13. Fernandez AM, Fernandez S, Carrero P, Garcia-Garcia M, Torres-Aleman I. Calcineurin in reactive astrocytes plays a key role in the interplay between proinflammatory and anti-inflammatory signals. J Neurosci. 2007; 27:8745–8756. DOI: 10.1523/JNEUROSCI.1002-07.2007 [PubMed: 17699657]
14. Sama MA, Mathis DM, Furman JL, Abdul HM, Artiushin IA, Kraner SD, Norris CM. Interleukin-1beta-dependent signaling between astrocytes and neurons depends critically on astrocytic calcineurin/NFAT activity. J Biol Chem. 2008; 283:21953–21964. DOI: 10.1074/jbc.M800148200 [PubMed: 18541537]
15. Fernandez AM, Hervas R, Dominguez-Fraile M, Garrido V, Gomez-Gutierrez P, Vega M, Vitorica J, Perez JJ, Torres Aleman I. Blockade of the Interaction of Calcineurin with FOXO in Astrocytes Protects Against Amyloid-beta-Induced Neuronal Death. J Alzheimers Dis. 2016; doi: 10.3233/JAD-160149
16. Fernandez AM, Jimenez S, Mecha M, Davila D, Guaza C, Vitorica J, Torres-Aleman I. Regulation of the phosphatase calcineurin by insulin-like growth factor I unveils a key role of astrocytes in Alzheimer's pathology. Mol Psychiatry. 2012; 17:705–718. DOI: 10.1038/mp.2011.128 [PubMed: 22005929]

17. Furman JL, Sompol P, Kraner SD, Pleiss MM, Putman EJ, Dunkerson J, Mohmmad Abdul H, Roberts KN, Scheff SW, Norris CM. Blockade of Astrocytic Calcineurin/NFAT Signaling Helps to Normalize Hippocampal Synaptic Function and Plasticity in a Rat Model of Traumatic Brain Injury. J Neurosci. 2016; 36:1502–1515. DOI: 10.1523/JNEUROSCI.1930-15.2016 [PubMed: 26843634]

18. Norris, CM. Calpain interactions with the protein phosphatase calcineurin in neurodegeneration. In: Dhalla, NS.; Chakraborti, S., editors. Role of Proteases in Cellular Dysfunction. Springer; New York, NY: 2014. p. 17-45.

19. Perrino BA, Ng LY, Soderling TR. Calcium regulation of calcineurin phosphatase activity by its B subunit and calmodulin. Role of the autoinhibitory domain. J Biol Chem. 1995; 270:340–346. [PubMed: 7814394]

20. Wu HY, Tomizawa K, Oda Y, Wei FY, Lu YF, Matsushita M, Li ST, Moriwaki A, Matsui H. Critical role of calpain-mediated cleavage of calcineurin in excitotoxic neurodegeneration. J Biol Chem. 2004; 279:4929–4940. DOI: 10.1074/jbc.M309767200 [PubMed: 14627704]

21. Huang W, Fileta JB, Dobberfuhl A, Filippopolous T, Guo Y, Kwon G, Grosskreutz CL. Calcineurin cleavage is triggered by elevated intraocular pressure, and calcineurin inhibition blocks retinal ganglion cell death in experimental glaucoma. Proc Natl Acad Sci U S A. 2005; 102:12242–12247. DOI: 10.1073/pnas.0505138102 [PubMed: 16103353]

22. Liu F, Grundke-Iqbal I, Iqbal K, Oda Y, Tomizawa K, Gong CX. Truncation and activation of calcineurin A by calpain I in Alzheimer disease brain. J Biol Chem. 2005; 280:37755–37762. DOI: 10.1074/jbc.M507475200 [PubMed: 16150694]

23. Rosenkranz K, May C, Meier C, Marcus K. Proteomic analysis of alterations induced by perinatal hypoxic-ischemic brain injury. J Proteome Res. 2012; 11:5794–5803. DOI: 10.1021/pr3005869 [PubMed: 23153068]

24. Shioda N, Han F, Moriguchi S, Fukunaga K. Constitutively active calcineurin mediates delayed neuronal death through Fas-ligand expression via activation of NFAT and FKHR transcriptional activities in mouse brain ischemia. J Neurochem. 2007; 102:1506–1517. DOI: 10.1111/j.1471-4159.2007.04600.x [PubMed: 17662023]

25. Shioda N, Moriguchi S, Shirasaki Y, Fukunaga K. Generation of constitutively active calcineurin by calpain contributes to delayed neuronal death following mouse brain ischemia. J Neurochem. 2006; 98:310–320. DOI: 10.1111/j.1471-4159.2006.03874.x [PubMed: 16805817]

26. Mohmmad Abdul H, Baig I, Levine H 3rd, Guttmann RP, Norris CM. Proteolysis of calcineurin is increased in human hippocampus during mild cognitive impairment and is stimulated by oligomeric Abeta in primary cell culture. Aging Cell. 2011; 10:103–113. doi:10.00645.x. DOI: 10.1111/j.1474-9726.20 [PubMed: 20969723]

27. Norris CM, Blalock EM, Thibault O, Brewer LD, Clodfelter GV, Porter NM, Landfield PW. Electrophysiological mechanisms of delayed excitotoxicity: positive feedback loop between NMDA receptor current and depolarization-mediated glutamate release. J Neurophysiol. 2006; 96:2488–2500. DOI: 10.1152/jn.00593.2005 [PubMed: 16914613]

28. Porter NM, Thibault O, Thibault V, Chen KC, Landfield PW. Calcium channel density and hippocampal cell death with age in long-term culture. J Neurosci. 1997; 17:5629–5639. [PubMed: 9204944]

29. Nelson PT, Jicha GA, Schmitt FA, Liu H, Davis DG, Mendiondo MS, Abner EL, Markesbery WR. Clinicopathologic correlations in a large Alzheimer disease center autopsy cohort: neuritic plaques and neurofibrillary tangles “do count” when staging disease severity. J Neuropathol Exp Neurol. 2007; 66:1136–1146. DOI: 10.1097/nen.0b013e31815c5efb [PubMed: 18090922]

30. Kincaid RL, Giri PR, Higuchi S, Tamura J, Dixon SC, Marietta CA, Amorese DA, Martin BM. Cloning and characterization of molecular isoforms of the catalytic subunit of calcineurin using nonisotopic methods. J Biol Chem. 1990; 265:11312–11319. [PubMed: 2162844]

31. Cui W, Mizukami H, Yanagisawa M, Aida T, Nomura M, Isomura Y, Takayanagi R, Ozawa K, Tanaka K, Aizawa H. Glial dysfunction in the mouse habenula causes depressive-like behaviors and sleep disturbance. J Neurosci. 2014; 34:16273–16285. DOI: 10.1523/JNEUROSCI.1465-14.2014 [PubMed: 25471567]

32. Ortinski PI, Dong J, Mungenast A, Yue C, Takano H, Watson DJ, Haydon PG, Coulter DA. Selective induction of astrocytic gliosis generates deficits in neuronal inhibition. Nat Neurosci. 2010; 13:584–91. [PubMed: 20418874]
33. Mathis DM, Furman JL, Norris CM. Preparation of acute hippocampal slices from rats and transgenic mice for the study of synaptic alterations during aging and amyloid pathology. J Vis Exp. 2011; doi: 10.3791/2330
34. Norris CM, Sompol P, Roberts KN, Ansari M, Scheff SW. Pycnogenol protects CA3-CA1 synaptic function in a rat model of traumatic brain injury. Exp Neurol. 2016; 276:5–12. DOI: 10.1016/j.expneurol.2015.11.006 [PubMed: 26607913]
35. Hashimoto Y, Perrino BA, Soderling TR. Identification of an autoinhibitory domain in calcineurin. J Biol Chem. 1990; 265:1924–1927. [PubMed: 2153670]
36. Celsi F, Svedberg M, Unger C, Cotman CW, Carri MT, Ottersen OP, Nordberg A, Torp R. Beta-amyloid causes downregulation of calcineurin in neurons through induction of oxidative stress. Neurobiol Dis. 2007; 26:342–352. DOI: 10.1016/j.nbd.2006.12.022 [PubMed: 17344052]
37. Goto S, Matsukado Y, Mihara Y, Inoue N, Miyamoto E. The distribution of calcineurin in rat brain by light and electron microscopic immunohistochemistry and enzyme-immunoassay. Brain Res. 1986; 397:161–172. [PubMed: 3542117]
38. Kuno T, Mukai H, Ito A, Chang CD, Kishima K, Saito N, Tanaka C. Distinct cellular expression of calcineurin A alpha and A beta in rat brain. J Neurochem. 1992; 58:1643–1651. [PubMed: 1313851]
39. Kromer Vogt LJ, Hyman BT, Van Hoesen GW, Damasio AR. Pathological alterations in the amygdala in Alzheimer's disease. Neuroscience. 1990; 37:377–385. [PubMed: 2133349]
40. Murphy GM Jr, Ellis WG, Lee YL, Stultz KE, Shrivastava R, Tinklenberg JR, Eng LF. Astrocytic gliosis in the amygdala in Down's syndrome and Alzheimer's disease. Prog Brain Res. 1992; 94:475–483. [PubMed: 1287731]
41. Kalaria RN, Akinyemi R, Ihara M. Does vascular pathology contribute to Alzheimer changes? J Neurol Sci. 2012; 322:141–147. DOI: 10.1016/j.jns.2012.07.032 [PubMed: 22884479]
42. Raz L, Knoefel J, Bhaskar K. The neuropathology and cerebrovascular mechanisms of dementia. J Cereb Blood Flow Metab. 2015; doi: 10.1038/jcbfm.2015.164
43. van Norden AG, van Dijk EJ, de Laat KF, Scheltens P, Olderikkert MG, de Leeuw FE. Dementia: Alzheimer pathology and vascular factors: from mutually exclusive to interaction. Biochim Biophys Acta. 2012; 1822:340–349. DOI: 10.1016/j.bbadis.2011.07.003 [PubMed: 21777675]
44. Vemuri P, Knopman DS. The role of cerebrovascular disease when there is concomitant Alzheimer disease. Biochim Biophys Acta. 2016; 1862:952–956. DOI: 10.1016/j.bbadis.2015.09.013 [PubMed: 26408957]
45. Corriveau RA, Bosetti F, Emr M, Gladman JT, Koenig JI, Moy CS, Pahigiannis K, Waddy SP, Koroshetz W. The Science of Vascular Contributions to Cognitive Impairment and Dementia (VCID): A Framework for Advancing Research Priorities in the Cerebrovascular Biology of Cognitive Decline. Cell Mol Neurobiol. 2016; 36:281–288. DOI: 10.1007/s10571-016-0334-7 [PubMed: 27095366]
46. Nelson AR, Sweeney MD, Sagare AP, Zlokovic BV. Neurovascular dysfunction and neurodegeneration in dementia and Alzheimer's disease. Biochim Biophys Acta. 2016; 1862:887–900. DOI: 10.1016/j.bbadis.2015.12.016 [PubMed: 26705676]
47. Wilcock DM, Schmitt FA, Head E. Cerebrovascular contributions to aging and Alzheimer's disease in Down syndrome. Biochim Biophys Acta. 2016; 1862:909–914. DOI: 10.1016/j.bbadis.2015.11.007 [PubMed: 26593849]
48. Kapasi A, Schneider JA. Vascular contributions to cognitive impairment, clinical Alzheimer's disease, and dementia in older persons. Biochim Biophys Acta. 2016; 1862:878–886. DOI: 10.1016/j.bbadis.2015.12.023 [PubMed: 26769363]
49. Smith EE, Schneider JA, Wardlaw JM, Greenberg SM. Cerebral microinfarcts: the invisible lesions. Lancet Neurol. 2012; 11:272–282. DOI: 10.1016/S1474-4422(11)70307-6 [PubMed: 22341035]
50. van Veluw SJ, Zwanenburg JJ, Rozemuller AJ, Luijten PR, Spliet WG, Biessels GJ. The spectrum of MR detectable cortical microinfarcts: a classification study with 7-tesla postmortem MRI and

histopathology. J Cereb Blood Flow Metab. 2015; 35:676–683. DOI: 10.1038/jcbfm.2014.258 [PubMed: 25605293]

51. Wang M, Iliff JJ, Liao Y, Chen MJ, Shinseki MS, Venkataraman A, Cheung J, Wang W, Nedergaard M. Cognitive deficits and delayed neuronal loss in a mouse model of multiple microinfarcts. J Neurosci. 2012; 32:17948–17960. DOI: 10.1523/JNEUROSCI.1860-12.2012 [PubMed: 23238711]
52. Grolla AA, Fakhfouri G, Balzaretti G, Marcello E, Gardoni F, Canonico PL, DiLuca M, Genazzani AA, Lim D. Abeta leads to Ca(2)(+) signaling alterations and transcriptional changes in glial cells. Neurobiol Aging. 2013; 34:511–522. DOI: 10.1016/j.neurobiolaging.2012.05.005 [PubMed: 22673114]
53. Jin SM, Cho HJ, Kim YW, Hwang JY, Mook-Jung I. Abeta-induced Ca(2+) influx regulates astrocytic BACE1 expression via calcineurin/NFAT4 signals. Biochem Biophys Res Commun. 2012; 425:649–655. DOI: 10.1016/j.bbrc.2012.07.123 [PubMed: 22846573]
54. Allen NJ. Astrocyte regulation of synaptic behavior. Annu Rev Cell Dev Biol. 2014; 30:439–463. DOI: 10.1146/annurev-cellbio-100913-013053 [PubMed: 25288116]
55. De Windt LJ, Lim HW, Taigen T, Wencker D, Condorelli G, Dorn GW 2nd, Kitsis RN, Molkentin JD. Calcineurin-mediated hypertrophy protects cardiomyocytes from apoptosis in vitro and in vivo: An apoptosis-independent model of dilated heart failure. Circ Res. 2000; 86:255–263. [PubMed: 10679475]
56. Friday BB, Horsley V, Pavlath GK. Calcineurin activity is required for the initiation of skeletal muscle differentiation. J Cell Biol. 2000; 149:657–666. [PubMed: 10791979]
57. Norris CM, Blalock EM, Chen KC, Porter NM, Thibault O, Kraner SD, Landfield PW. Hippocampal 'zipper' slice studies reveal a necessary role for calcineurin in the increased activity of L-type Ca(2+) channels with aging. Neurobiol Aging. 2010; 31:328–338. DOI: 10.1016/j.neurobiolaging.2008.03.026 [PubMed: 18471936]
58. Wang HG, Pathan N, Ethell IM, Krajewski S, Yamaguchi Y, Shibasaki F, McKeon F, Bobo T, Franke TF, Reed JC. Ca2+-induced apoptosis through calcineurin dephosphorylation of BAD. Science. 1999; 284:339–343. [PubMed: 10195903]
59. Billingsley ML, Ellis C, Kincaid RL, Martin J, Schmidt ML, Lee VM, Trojanowski JQ. Calcineurin immunoreactivity in Alzheimer's disease. Exp Neurol. 1994; 126:178–184. DOI: 10.1006/exnr.1994.1056 [PubMed: 7925818]
60. Ladner CJ, Czech J, Maurice J, Lorens SA, Lee JM. Reduction of calcineurin enzymatic activity in Alzheimer's disease: correlation with neuropathologic changes. J Neuropathol Exp Neurol. 1996; 55:924–931. [PubMed: 8759782]
61. Lian Q, Ladner CJ, Magnuson D, Lee JM. Selective changes of calcineurin (protein phosphatase 2B) activity in Alzheimer's disease cerebral cortex. Exp Neurol. 2001; 167:158–165. DOI: 10.1006/exnr.2000.7534 [PubMed: 11161603]
62. Karch CM, Jeng AT, Goate AM. Calcium phosphatase calcineurin influences tau metabolism. Neurobiol Aging. 2013; 34:374–386. DOI: 10.1016/j.neurobiolaging.2012.05.003 [PubMed: 22676853]
63. Hashimoto T, Kawamata T, Saito N, Sasaki M, Nakai M, Niu S, Taniguchi T, Terashima A, Yasuda M, Maeda K, Tanaka C. Isoform-specific redistribution of calcineurin A alpha and A beta in the hippocampal CA1 region of gerbils after transient ischemia. J Neurochem. 1998; 70:1289–1298. [PubMed: 9489752]
64. Hamby ME, Sofroniew MV. Reactive astrocytes as therapeutic targets for CNS disorders. Neurotherapeutics. 2010; 7:494–506. DOI: 10.1016/j.nurt.2010.07.003 [PubMed: 20880511]
65. Pekny M, Pekna M. Astrocyte reactivity and reactive astrogliosis: costs and benefits. Physiol Rev. 2014; 94:1077–1098. DOI: 10.1152/physrev.00041.2013 [PubMed: 25287860]
66. Verkhratsky A, Sofroniew MV, Messing A, deLanerolle NC, Rempe D, Rodriguez JJ, Nedergaard M. Neurological diseases as primary gliopathies: a reassessment of neurocentrism. ASN Neuro. 2012; 4doi: 10.1042/AN20120010
67. Verkhratsky A, Steardo L, Parpura V, Montana V. Translational potential of astrocytes in brain disorders. Prog Neurobiol. 2015; doi: 10.1016/j.pneurobio.2015.09.003

68. Kim B, Jeong HK, Kim JH, Lee SY, Jou I, Joe EH. Uridine 5′-diphosphate induces chemokine expression in microglia and astrocytes through activation of the P2Y6 receptor. J Immunol. 2011; 186:3701–3709. DOI: 10.4049/jimmunol.1000212 [PubMed: 21317391]
69. Nagamoto-Combs K, Combs CK. Microglial phenotype is regulated by activity of the transcription factor, NFAT (nuclear factor of activated T cells). J Neurosci. 2010; 30:9641–9646. DOI: 10.1523/JNEUROSCI.0828-10.2010 [PubMed: 20631193]
70. Shiratori M, Tozaki-Saitoh H, Yoshitake M, Tsuda M, Inoue K. P2X7 receptor activation induces CXCL2 production in microglia through NFAT and PKC/MAPK pathways. J Neurochem. 2010; 114:810–819. DOI: 10.1111/j.1471-4159.2010.06809.x [PubMed: 20477948]
71. Filosa JA, Nelson MT, Gonzalez Bosc LV. Activity-dependent NFATc3 nuclear accumulation in pericytes from cortical parenchymal microvessels. Am J Physiol Cell Physiol. 2007; 293:C1797–1805. DOI: 10.1152/ajpcell.00554.2006 [PubMed: 17881610]
72. Shih AY, Blinder P, Tsai PS, Friedman B, Stanley G, Lyden PD, Kleinfeld D. The smallest stroke: occlusion of one penetrating vessel leads to infarction and a cognitive deficit. Nat Neurosci. 2013; 16:55–63. DOI: 10.1038/nn.3278 [PubMed: 23242312]
73. Bachstetter AD, Norris CM, Sompol P, Wilcock DM, Goulding D, Neltner JH, St Clair D, Watterson DM, Van Eldik LJ. Early stage drug treatment that normalizes proinflammatory cytokine production attenuates synaptic dysfunction in a mouse model that exhibits age-dependent progression of Alzheimer's disease-related pathology. J Neurosci. 2012; 32:10201–10210. DOI: 10.1523/JNEUROSCI.1496-12.2012 [PubMed: 22836255]
74. Rossi D. Astrocyte physiopathology: At the crossroads of intercellular networking, inflammation and cell death. Prog Neurobiol. 2015; 130:86–120. DOI: 10.1016/j.pneurobio.2015.04.003 [PubMed: 25930681]
75. Griffin WS, Sheng JG, Royston MC, Gentleman SM, McKenzie JE, Graham DI, Roberts GW, Mrak RE. Glial-neuronal interactions in Alzheimer's disease: the potential role of a 'cytokine cycle' in disease progression. Brain Pathol. 1998; 8:65–72. [PubMed: 9458167]
76. Mrak RE, Griffin WS. Glia and their cytokines in progression of neurodegeneration. Neurobiol Aging. 2005; 26:349–354. DOI: 10.1016/j.neurobiolaging.2004.05.010 [PubMed: 15639313]
77. Van Eldik LJ, Thompson WL, Ralay Ranaivo H, Behanna HA, Martin Watterson D. Glia proinflammatory cytokine upregulation as a therapeutic target for neurodegenerative diseases: function-based and target-based discovery approaches. Int Rev Neurobiol. 2007; 82:277–296. DOI: 10.1016/S0074-7742(07)82015-0 [PubMed: 17678967]
78. Pickering M, O'Connor JJ. Pro-inflammatory cytokines and their effects in the dentate gyrus. Prog Brain Res. 2007; 163:339–354. DOI: 10.1016/S0079-6123(076)3020-9 [PubMed: 17765728]
79. Sama DM, Norris CM. Calcium dysregulation and neuroinflammation: discrete and integrated mechanisms for age-related synaptic dysfunction. Ageing Res Rev. 2013; 12:982–995. DOI: 10.1016/j.arr.2013.05.008 [PubMed: 23751484]
80. Jones EV, Bernardinelli Y, Tse YC, Chierzi S, Wong TP, Murai KK. Astrocytes control glutamate receptor levels at developing synapses through SPARC-beta-integrin interactions. J Neurosci. 2011; 31:4154–4165. DOI: 10.1523/JNEUROSCI.4757-10.2011 [PubMed: 21411656]
81. Murai KK, Pasquale EB. Eph receptors and ephrins in neuron-astrocyte communication at synapses. Glia. 2011; 59:1567–1578. DOI: 10.1002/glia.21226 [PubMed: 21850709]
82. Stevens B, Allen NJ, Vazquez LE, Howell GR, Christopherson KS, Nouri N, Micheva KD, Mehalow AK, Huberman AD, Stafford B, Sher A, Litke AM, Lambris JD, Smith SJ, John SW, Barres BA. The classical complement cascade mediates CNS synapse elimination. Cell. 2007; 131:1164–1178. DOI: 10.1016/j.cell.2007.10.036 [PubMed: 18083105]
83. Frugier T, Conquest A, McLean C, Currie P, Moses D, Goldshmit Y. Expression and activation of EphA4 in the human brain after traumatic injury. J Neuropathol Exp Neurol. 2012; 71:242–250. DOI: 10.1097/NEN.0b013e3182496149 [PubMed: 22318127]
84. Ingram G, Loveless S, Howell OW, Hakobyan S, Dancey B, Harris CL, Robertson NP, Neal JW, Morgan BP. Complement activation in multiple sclerosis plaques: an immunohistochemical analysis. Acta Neuropathol Commun. 2014; 2:53.doi: 10.1186/2051-5960-2-53 [PubMed: 24887075]

85. Ridet JL, Malhotra SK, Privat A, Gage FH. Reactive astrocytes: cellular and molecular cues to biological function. Trends Neurosci. 1997; 20:570–577. [PubMed: 9416670]

86. Scheff SW, Price DA, Ansari MA, Roberts KN, Schmitt FA, Ikonomovic MD, Mufson EJ. Synaptic change in the posterior cingulate gyrus in the progression of Alzheimer's disease. J Alzheimers Dis. 2015; 43:1073–1090. DOI: 10.3233/JAD-141518 [PubMed: 25147118]

87. Scheff SW, Price DA, Schmitt FA, Roberts KN, Ikonomovic MD, Mufson EJ. Synapse stability in the precuneus early in the progression of Alzheimer's disease. J Alzheimers Dis. 2013; 35:599–609. DOI: 10.3233/JAD-122353 [PubMed: 23478309]

88. Scheff SW, Ansari MA, Mufson EJ. Oxidative stress and hippocampal synaptic protein levels in elderly cognitively intact individuals with Alzheimer's disease pathology. Neurobiol Aging. 2016; 42:1–12. DOI: 10.1016/j.neurobiolaging.2016.02.030 [PubMed: 27143416]

89. Sinclair LI, Tayler HM, Love S. Synaptic protein levels altered in vascular dementia. Neuropathol Appl Neurobiol. 2015; 41:533–543. DOI: 10.1111/nan.12215 [PubMed: 25559750]

90. Foster TC, Sharrow KM, Masse JR, Norris CM, Kumar A. Calcineurin links Ca2+ dysregulation with brain aging. J Neurosci. 2001; 21:4066–4073. [PubMed: 11356894]

91. Taglialatela G, Hogan D, Zhang WR, Dineley KT. Intermediate- and long-term recognition memory deficits in Tg2576 mice are reversed with acute calcineurin inhibition. Behav Brain Res. 2009; 200:95–99. DOI: 10.1016/j.bbr.2008.12.034 [PubMed: 19162087]

92. Kuchibhotla KV, Goldman ST, Lattarulo CR, Wu HY, Hyman BT, Bacskai BJ. Abeta plaques lead to aberrant regulation of calcium homeostasis in vivo resulting in structural and functional disruption of neuronal networks. Neuron. 2008; 59:214–225. DOI: 10.1016/j.neuron.2008.06.008 [PubMed: 18667150]

93. Hudry E, Wu HY, Arbel-Ornath M, Hashimoto T, Matsouaka R, Fan Z, Spires-Jones TL, Betensky RA, Bacskai BJ, Hyman BT. Inhibition of the NFAT pathway alleviates amyloid beta neurotoxicity in a mouse model of Alzheimer's disease. J Neurosci. 2012; 32:3176–3192. DOI: 10.1523/JNEUROSCI.6439-11.2012 [PubMed: 22378890]

Highlights

- Study used a novel antibody for identifying proteolyzed, active calcineurin
- Calcineurin proteolysis appeared in astrocytes of human Alzheimer's disease brain
- Antibody labeling was very intense around amyloid plaques and microinfarcts
- AAV expression of active calcineurin in astrocytes caused synaptic deficits in rats
- Calcineurin proteolysis is a key pathogenic mechanism resulting in synaptic alterations

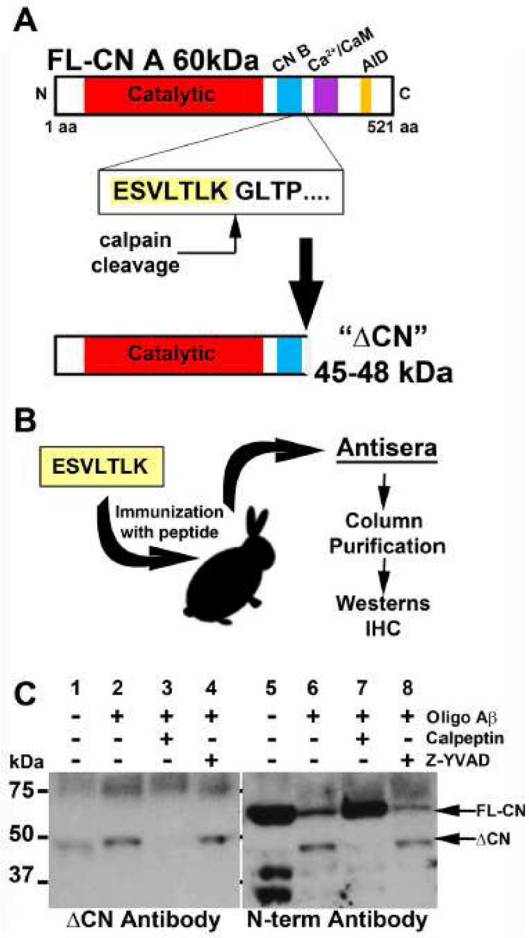

Figure 1. Production of ΔCN antibody

(**A**) Calpain-dependent cleavage between lysine 424 and glycine 425 generates a 45–48 kDa fragment (ΔCN). (**B**) The peptide immediately upstream from the ΔCN cleavage site (ESVLTLK) was used to immunize rabbits. Antisera was column-purified to enrich the ΔCN antibody. (**C**) Western blot showing proteolysis of CN in primary rat hippocampal cultures treated for 24 h with oligomeric Aβ1-42 peptides (65 nM) in the presence or absence of the CP inhibitor, calpeptin (10μM) or caspase-1 inhibitor, Z-YVAD. The ΔCN antibody (left panel) detects the 45–48 kDa fragment but not full-length CN. Commercial N terminus antibodies (right panel) recognize both full-length (60 kDa) CN and the 45–48 kDa fragment. Blockade of CP activity with calpeptin prevents Aβ-dependent proteolysis while inhibition of caspase activity does not.

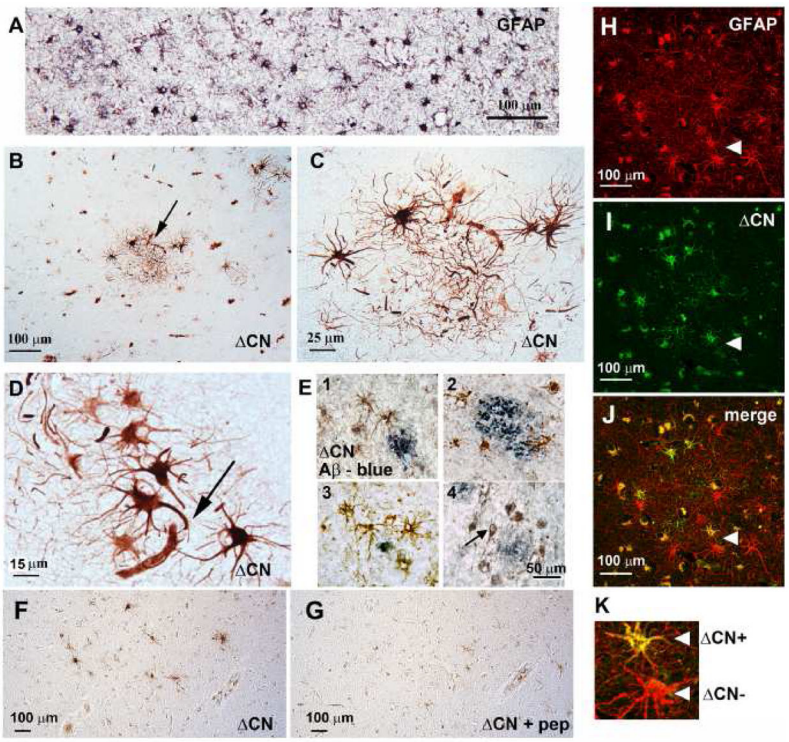

Figure 2. ΔCN antibody labels astrocytes in human tissue

(**A**) GFAP labeling in an AD section from a subject with confirmed AD. (**B–C**) Low and high power photomicrographs of human AD amygdala showing intense labeling of astrocyte clusters and (**D**) astrocytes in close proximity to microvessels using the ΔCN antibody. (**E1–4**) Co-labeling reveals that ΔCN-positive cells (brown) appear around amyloid deposits (blue). Though most cells contained within clusters exhibited a clear astrocyte morphology, some cells showed neuron-like characteristics (see arrow in **E4**). (**F,G**) Serial sections of amygdala labeled with ΔCN antibody alone (F) or ΔCN antibody plus ESVLTLK blocking peptide (**G**). (**H–K**) Confocal micrographs showing labeling with a GFAP antibody (red) and the ΔCN antibody (green). The merged image shows areas of colocalization, indicating that most GFAP-positive astrocytes have regions that are also occupied by the ΔCN fragment (arrows). However; some GFAP-positive astrocytes (indicated by arrowheads and shown at larger magnification in **K**) were devoid of ΔCN.

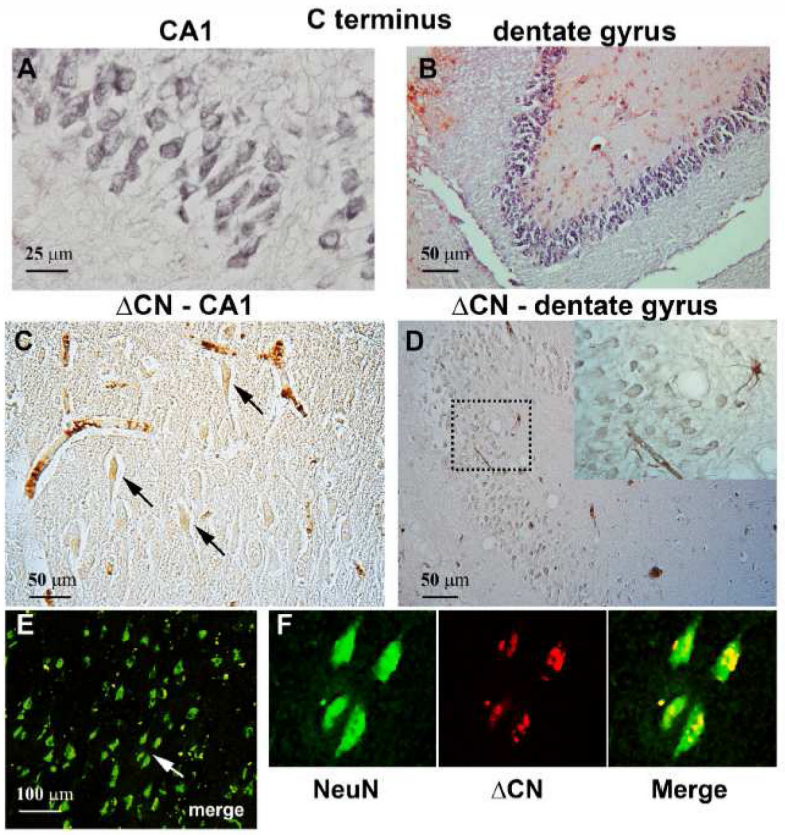

Figure 3. ΔCN antibody shows faint labeling in NeuN positive neurons

(**A–B**) Photomicrographs of human AD hippocampus in CA1 (**A**) and in the dentate gyrus (**B**) show strong labeling of neurons using a commercial antibody to the C-terminus of CN. (**C–D**) Labeling of the CA1 and dentate granule layers with the ΔCN antibody. Neuronal labeling with the ΔCN antibody was relatively faint and limited to the cell body region and proximal apical dendrites (for pyramidal neurons). Inset in **D** shows an intesely labeled astrocyte and blood vessel near weakly labeled dentate granule cells. (**E–F**) Low (**E**) and higher-powered (**F**) confocal micrographs of NeuN and ΔCN double-labeling in area CA1 of an AD subject. Merged low-power images from the region denoted by the arrow in panel **E** shows punctate localization of ΔCN (red) to NeuN positve cell bodies (green).

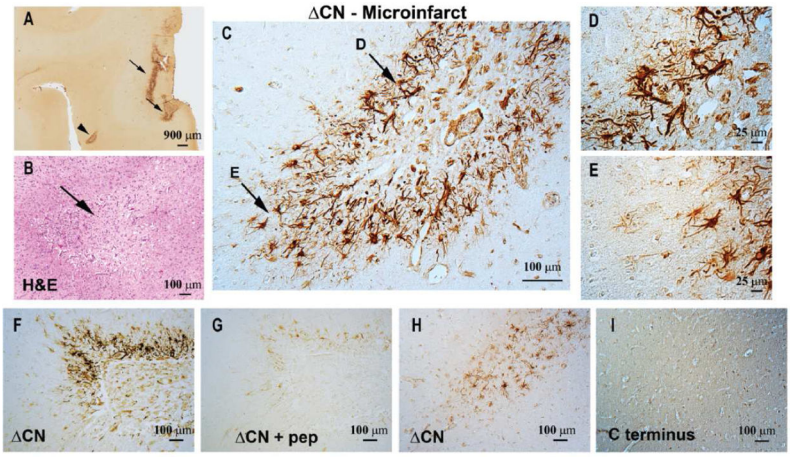

Figure 4. ΔCN antibody labels microinfarcts

Representative low magnification photomicrograph (**A**) that shows ΔCN labeling around several microinfarcts (arrows and arrowhead) in neocortex. (**B**) Serial section through neocortex stained by H&E to confirm the presence of microinfarcts. The image shown is a high magnification of the region denoted by the arrowhead in Panel **A**. (**C**) High power photomicrograph of the region in **A** (arrowhead) showing intense ΔCN antibody labeling of astrocytes. Higher magnification of the areas denoted by arrows are shown in panels **D** and **E**. (**F**,**G**) Serial sections of neocortex labeled with ΔCN antibody alone (**F**) or ΔCN antibody plus ESVLTLK blocking peptide (**G**). The blocking peptide greatly reduced the labeling intensity of the ΔCN antibody. (**H,I**) Serial sections of human cortical tissue treated with the ΔCN antibody (**H**), or a commercial C-terminus antibody (**I**) that detects FL-CN, but not proteolyzed CN (**G**). Little to no labeling in the microinfarct region is observed with the C-terminus antibody.

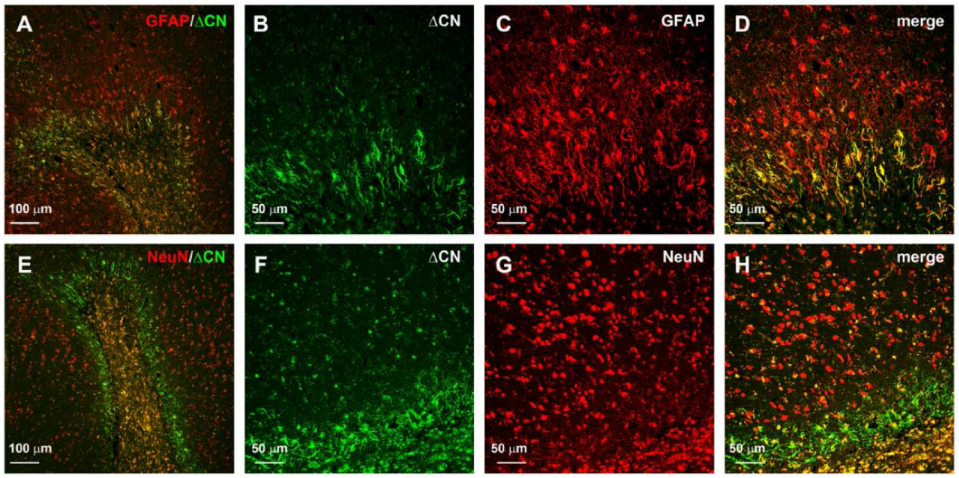

Figure 5. ΔCN localizes to astrocytes and neurons around microinfarcts

(**A**) Merged confocal micrograph showing the colocalization of ΔCN (green) with GFAP (red). **B**–**D**, high magnification images of the infarct in Panel A shown in individual channels (**B**,**C**) and merged (**D**). Co-localization of ΔCN with GFAP was most extensive in the region immediately adjacent to the infarct. (**E**) Merged confocal micrograph showing the colocalization of ΔCN (green) with NeuN (red). Note, this image is a serial section of the reigion shown in Panel **A. F**–**H**, high magnification images of the infarct in Panel E shown in individual channels (**F**,**G**) and merged (**H**). Co-localization of ΔCN with NeuN was most extensive in the microinfarct core, but could also be observed for numerous cells adjacent to the insult.

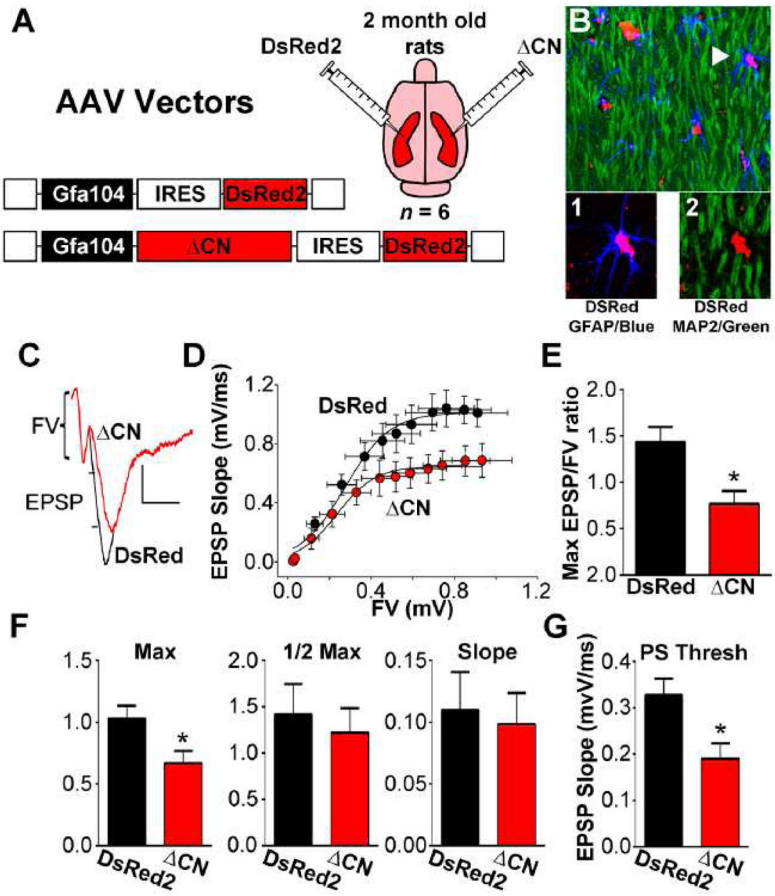

Figure 6. ΔCN expression and hippocampal synaptic function

(**A**) AAV2/5 vectors encoding a DsRed2 control construct or a ΔCN construct under the control of the astrocyte-specific promoter, Gfa104, were injected into alternate hemispheres (intrahippocampal) of intact adult rats (n =6). **B**, Confocal micrograph of the stratum radiatum region of area CA1 showing MAP2b (green), GFAP (blue), and DsRed2 (red). Arrow points to a DsRed2-positive astrocyte shown in higher magnigfication images below. While many astrocytes labeled positive for DsRed2, there was no overlap in labeling for DsRed2 and MAP2b. **C**, representative waveforms recorded in *stratum radiatum* of CA1 in response to electrical orthodromic stimulation of Schaffer collaterals illustrating a reduced EPSP in slices from the the ΔCN-treated hemisphere relative to the DsRed2-treated hemisphere, given a similar FV amplitude. Calibration bars: vertical 0.5 mV; horizontal 5 msec. **D**, Synaptic strength curves showing the mean ± SEM EPSP slope values plotted against the mean ± SEM FV amplitude values at increasing stimulus intensities. The average synaptic strength curve for the ΔCN-treated hemisphere exhibited a downward shift, consistent with reduced basal synaptic strength. **E**, Mean ± SEM maximal EPSP-to-FV ratio in each AAV-treated hemisphere. **F**, Synaptic strength curve parameters (Mean ± SEM maximal EPSP, curve slope, and half-maximal activation) from the data shown in panel **C.** **G**, Mean ± SEM PS threshold in ΔCN- and DsRed2-treated slices. *p<0.05, paired t-test.